Complex magnetic phase diagram with multistep spin-flop transitions in $La_{0.25}Pr_{0.75}Co_2P_2$

Xiaoyan Tan,[1,*] V. Ovidiu Garlea,[2,†] Kirill Kovnir,[1,‡] Corey M. Thompson,[1,§] Tongshuai Xu,[3] Huibo Cao,[2] Ping Chai,[1] Zachary P. Tener,[1] Shishen Yan,[3] Peng Xiong,[4] and Michael Shatruk[1,†]

[1]*Department of Chemistry and Biochemistry, Florida State University, Tallahassee, Florida 32306, USA*

[2]*Quantum Condensed Matter Division, Oak Ridge National Laboratory, Oak Ridge, Tennessee 37831, USA*

[3]*School of Physics, National Key Laboratory of Crystal Materials, Shandong University, Jinan, Shandong, 250100, People's Republic of China*

[4]*Department of Physics, Florida State University, Tallahassee, Florida 32306, USA*

(Received 11 August 2016; revised manuscript received 13 December 2016; published 24 January 2017)

$La_{0.25}Pr_{0.75}Co_2P_2$ crystallizes in the tetragonal $ThCr_2Si_2$ structure type and shows multiple magnetic phase transitions driven by changes in temperature and magnetic field. The nature of these transitions was investigated by a combination of magnetic and magnetoresistance measurements and both single crystal and powder neutron diffraction. The Co magnetic moments order ferromagnetically (FM) parallel to the *c* axis at 282 K, followed by antiferromagnetic (AFM) ordering at 225 K. In the AFM structure, the Co magnetic moments align along the *c* axis with FM $[Co_2P_2]$ layers arranged in an alternating sequence, $\uparrow\uparrow\downarrow\downarrow$, which leads to the doubling of the *c* axis in the magnetic unit cell. Another AFM transition is observed at 27 K, due to the ordering of a half of Pr moments in the *ab* plane. The other half of Pr moments undergoes AFM ordering along the *c* axis at 11 K, causing simultaneous reorientation of the previously ordered Pr moments into an AFM structure with the moments being canted with respect to the *c* axis. This AFM transition causes an abrupt decrease in electrical resistivity at 11 K. Under applied magnetic field, two metamagnetic transitions are observed in the Pr sublattice at 0.8 and 5.4 T. They correlate with two anomalies in magnetoresistance measurements at the same critical fields. A comparison of the temperature- and field-dependent magnetic properties of $La_{0.25}Pr_{0.75}Co_2P_2$ to the magnetic behavior of $PrCo_2P_2$ is provided.

DOI: 10.1103/PhysRevB.95.024428

I. INTRODUCTION

AT_2X_2 compounds with layered $ThCr_2Si_2$-type structure, where *A* is a rare earth, alkaline earth, or alkali metal, *T* is a transition metal, and *X* is a metalloid element, represent a large class of materials with long-standing interest in their structural, transport, and magnetic properties [1–5]. This interest was reinvigorated by the discovery of iron-based high-temperature superconductors in 2008 [6]. Superconductivity is believed to originate in the $[T_2X_2]$ layer via suppression of the antiferromagnetic (AFM) order through carrier doping induced by chemical substitution or applied pressure [7]. Furthermore, superconductivity is found to coexist with large rare-earth magnetic moments in some AFM compounds of this class, e.g., $Eu_{0.5}K_{0.5}Fe_2As_2$ and $Eu_{0.7}Na_{0.3}Fe_2As_2$ [8,9].

The RCo_2P_2 (R = La–Sm) compounds are an intriguing subgroup of the AT_2X_2 materials. Their structural and magnetic properties were studied extensively, especially by Jeitschko *et al.* in 1980s [10], who also established the magnetic structures of these compounds by neutron diffraction studies in 1990s [11–13]. While $LaCo_2P_2$ was found to exhibit ferromagnetic (FM) ordering of Co moments in the *ab* plane at 125 K [Fig. 1(a)], the other compounds of this series exhibit AFM ordering of Co moments along the *c* axis around room temperature [Fig. 1(b)]. The R moments also undergo AFM ordering, but at much lower temperatures (e.g., $T_N^{Pr} = 19$K). Thus, due to the cancellation of Co spin at higher temperatures, the magnetic phase transitions in the $4f$ and $3d$ sublattices are "decoupled," which prevents the direct assessment of the $3d$-$4f$ exchange interactions in these materials.

Our recent studies, however, have demonstrated that substitutions into the R or Co sublattices lead to complex magnetic behavior, with coexistence of different magnetically ordered states [14–17]. For instance, given the drastically different magnetic behavior of the FM $LaCo_2P_2$ and AFM $PrCo_2P_2$ materials, the substitution of Pr for La provides a straightforward route to modulating the exchange interactions in order to produce novel magnetic and magnetotransport properties. Indeed, our previous studies of $La_{1-x}Pr_xCo_2P_2$ showed the presence of multiple magnetic transitions in these mixed phases [14]. We found that the FM ordering temperature for the Co sublattice gradually increases with increasing Pr content (x), from 132 K for $LaCo_2P_2$ to as high as 268 K for $La_{0.25}Pr_{0.75}Co_2P_2$. The preservation of the FM ordering of Co moments exerts a substantial effect on the magnetic behavior of the R sublattice. A detailed investigation of $La_{0.75}Pr_{0.25}Co_2P_2$ demonstrated three consecutive magnetic transitions, starting with FM ordering of Co moments at 167 K, ferrimagnetic (FiM) ordering with nearly antiparallel alignment of Pr and Co moments at 70 K, and a spin reorientation transition leading to collinear FiM ordering at 35 K [16]. We note the remarkable increase in the ordering temperature of the Pr sublattice as compared to that observed for the unsubstituted $PrCo_2P_2$. Nevertheless, the Pr-rich $La_{1-x}Pr_xCo_2P_2$ samples also showed an emergence of a significant AFM component, which makes them quite different from $La_{0.75}Pr_{0.25}Co_2P_2$.

*Present address: Department of Chemistry and Chemical Biology, Rutgers, the State University of New Jersey, 610 Taylor Rd, Piscataway, NJ 08854, USA.

†Corresponding authors: shatruk@chem.fsu.edu, garleao@ornl.gov

‡Present address: Department of Chemistry, University of California, Davis, One Shields Ave, Davis, CA 95616, USA.

§Present address: Department of Chemistry, Purdue University, 560 Oval Dr, West Lafayette, IN 47907, USA.

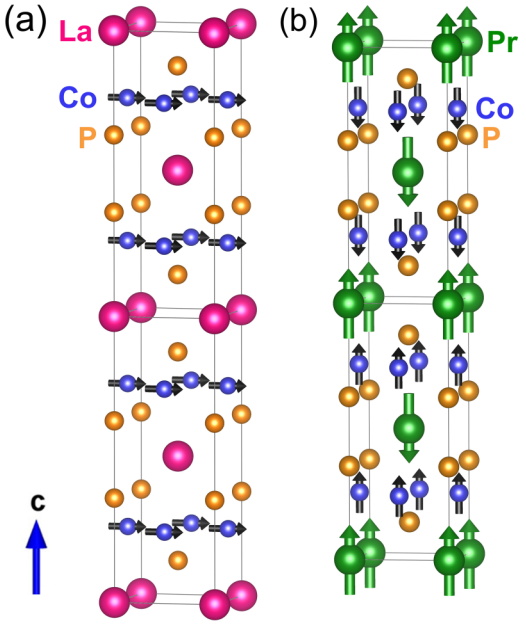

FIG. 1. (a) Magnetic structures of $LaCo_2P_2$ (showing two unit cells) and (b) $PrCo_2P_2$, according to Refs. [10] and [13].

In the present work, we set out to perform a detailed study of $La_{0.25}Pr_{0.75}Co_2P_2$. Herein we report the results of magnetization and magnetoresistance (MR) measurements performed on an oriented single crystals of $La_{0.25}Pr_{0.75}Co_2P_2$, as well as investigation of magnetic ordering in this material by means of neutron diffraction. In addition, we report the magnetic structure of $PrCo_2P_2$ under applied magnetic field and compare it to the magnetic structure of $La_{0.25}Pr_{0.75}Co_2P_2$. We demonstrate the high sensitivity of magnetoresistance measurements to the spin-flop transitions in these materials. Controlling the spin flop and resulting magnetoresistance by modulating the exchange coupling may offer a useful approach to the engineering of new spintronic materials.

II. EXPERIMENTAL METHODS

Finely dispersed powders of lanthanum (99.9%), praseodymium (99.9%), and red phosphorus (99.99%), as well as tin shots (99.99%), were obtained from Alfa Aesar and used as received. Cobalt powder (Alfa Aesar, 99.5%) was additionally purified by heating under a flow of H_2 gas at 775 K for 5 h. All manipulations during sample preparation were carried out in an argon-filled dry box (content of $O_2 < 1$ ppm).

$La_{0.25}Pr_{0.75}Co_2P_2$ was prepared by annealing a mixture of elements in tin flux as reported earlier [14]. Large platelike single crystals ($1 \times 1 \times 0.1\,mm^3$) were selected for physical properties measurements. The La/Pr ratio of 0.25:0.75 was confirmed by energy-dispersive x-ray microanalysis on a JEOL 5900 scanning electron microscope.

Magnetic measurements were performed on an oriented single crystal with a Quantum Design SQUID magnetometer MPMS-XL. Direct current magnetic susceptibility measurements were carried out in an applied field of 10 mT in the temperature range of 1.8–300 K. Isothermal field dependences of magnetization were measured with the magnetic field varying between 0 and 7 T.

Electrical transport measurements were conducted on an oriented single crystal in an Oxford ^{3}He system with the Van der Pauw configuration. The ac current was applied in the ab plane and the obtained voltage was measured by lock-in detection. The magnetic field was applied within the ab plane or along the c axis.

Powder and single-crystal neutron diffraction experiments on $La_{0.25}Pr_{0.75}Co_2P_2$ were carried out using the HB-2A high-resolution powder diffractometer [18] and the HB-3A four-circle diffractometer [19] at the High Flux Isotope Reactor at Oak Ridge National Laboratory. For the powder diffraction measurements we employed 1.546-Å and 2.410-Å neutron wavelengths that were produced by (115) and (113) reflections, respectively, from a vertically focusing Ge monochromator. Measurements were performed on a sample of ~8 g held in a cylindrical vanadium container placed in a top-loading closed cycle refrigerator, covering a temperature range of 4–300 K. Measurements under applied magnetic field from 0 to 7 T were performed on pelletized samples, to avoid reorientation of the crystallites. The data were collected by scanning the detector array consisting of 44 ^{3}He tubes in two segments, to cover the total 2θ range of 7°–133° in steps of 0.05°. Rietveld refinement of the collected data was carried out using FULLPROF software [20]. An analysis of symmetry-allowed magnetic models was performed using SARAh representational analysis software [21] and MAXMAGN at the Bilbao crystallographic server [22].

The single-crystal neutron diffraction experiment was performed on a large single crystal of $La_{0.25}Pr_{0.75}Co_2P_2$ ($3.0 \times 1.5 \times 0.1\,mm^3$). The neutron wavelength of 1.546 Å was generated from a bent silicon crystal monochromator. The data were collected at 4.5, 11, 200, and 300 K. Several selected magnetic peaks were measured as a function of temperature to determine the magnetic ordering temperature.

III. RESULTS AND DISCUSSIONS

A. Crystal structure

As shown in our earlier report, $La_{0.25}Pr_{0.75}Co_2P_2$ has a $ThCr_2Si_2$-type structure, space group $I4/mmm$ [14]. The structure contains layers of R atoms and $[Co_2P_2]$ slabs alternating along the c axis (Fig. 1). The structure was confirmed by high-resolution neutron diffraction experiments performed in the 4–300 K temperature range. Rietveld refinement of the neutron diffraction patterns revealed that the unit cell parameter a slightly increases as the temperature is lowered, but the parameter c decreases to a larger extent, thus causing the overall decrease in the unit cell volume (Table I). Below 30 K, the unit cell parameters remain essentially constant.

In our earlier reports, it was shown that the magnetic properties of RCo_2P_2 are related to the intralayer Co-Co distance, which is also correlated with the interlayer P-P separation. The substitution of La for Pr in $PrCo_2P_2$ results in shorter d(Co-Co) and longer d(P-P) values [14]. In this structure type, $d(\text{Co-Co}) = a/\sqrt{2}$, while d(P-P) is related to the unit cell parameter c and the z coordinate of the Wyckoff position 4e (0,0,z). The d(Co-Co) value in the structure of $La_{0.25}Pr_{0.75}Co_2P_2$ increases as the temperature is lowered from 300 K to 225 K and continues to increase, albeit only slightly, upon further temperature decrease. The d(P-P), however, does

TABLE I. Crystal structure parameters of $La_{0.25}Pr_{0.75}Co_2P_2$ determined by powder neutron diffraction ($\lambda = 2.410$ Å).

T (K)	a(Å) c(Å)	V(Å^3)	d(Co-Co)(Å)	d(P-P)(Å)
300	3.9012(1) 9.8918(5)	150.550(8)	2.7586(7)	2.65(2)
225	3.90586(4) 9.8142(4)	149.724(6)	2.76186(3)	2.65(1)
100	3.90654(7) 9.7605(3)	148.956(6)	2.76234(5)	2.58(1)
30	3.90694(7) 9.7476(3)	148.789(6)	2.76262(5)	2.59(1)
10	3.90699(7) 9.7489(3)	148.814(6)	2.76266(5)	2.59(1)
4	3.90682(7) 9.7453(3)	148.745(5)	2.76254(5)	2.59(1)

not change between 300 K and 225 K but exhibits a decrease when the temperature is lowered to 100 K (Table I).

B. Magnetic properties

The magnetic measurements were carried out on an oriented single crystal of $La_{0.25}Pr_{0.75}Co_2P_2$, with a magnetic field of 0.01 T applied parallel or perpendicular to the tetragonal c axis. The magnetic susceptibility measured with $H||c$ ($\chi_{||}$) exceeds by an order of magnitude the values measured with $H\perp c$ ($\chi_\perp$), which indicates the c axis to be the easy magnetization direction (Fig. 2). The temperature dependence of $\chi_{||}$ measured in the field-cooled mode reveals three magnetic phase transitions. The first one is observed as an abrupt increase in the $\chi_{||}$ values at $T_{C1} = 282$ K, where one also observes the divergence between the field-cooled (FC) and zero-field-cooled (ZFC) magnetization curves (see Fig. S1(a) in Ref. [23]). By comparison to the behavior of $La_{1-x}Pr_xCo_2P_2$ with $x = 0$, 0.25, and 0.50, in which such an increase is observed at 132, 167, and 200 K, respectively [14,16], we attribute this feature to the FM ordering of Co magnetic moments along the c axis. The ordering temperature also agrees with the Weiss constant of 283(4) K obtained from the Curie-Weiss fit of the high-temperature part for the $1/\chi_{||}$ versus T curve (see Fig. S1(b) in Ref. [23]). This high-temperature magnetic ordering is different from that observed for $LaCo_2P_2$ or $La_{0.75}Pr_{0.25}Co_2P_2$, in which the Co moments exhibit FM ordering in the ab plane at 132 and 167 K, respectively. Thus, while the easy magnetization direction for ordered Co moments in $La_{0.75}Pr_{0.25}Co_2P_2$ is reminiscent of that observed in the unsubstituted $LaCo_2P_2$, the easy magnetization direction in $La_{0.25}Pr_{0.75}Co_2P_2$ is the same as in $PrCo_2P_2$ (Fig. 1).

The second magnetic phase transition is seen as a peak in the $\chi_{||}$ value with the onset around 250 K and the maximum at $T_{C2} = 225$ K, which is probably associated with the reorientation of Co moments to adopt an AFM ordered state, similar to the behavior observed in pure $PrCo_2P_2$. The $\chi_{||}$ values exhibit a gradual decrease and approach zero around 30 K. Below this temperature, the $\chi_{||}$ increases abruptly to reach a sharp peak at $T_{N3} = 11$ K. A similar feature is observed in the $\chi_\perp$ curve. By comparing the magnetic behavior of $La_{0.25}Pr_{0.75}Co_2P_2$ to that of $PrCo_2P_2$ [10], we might expect that this third phase involves AFM ordering of Pr moments.

Isothermal field dependences of magnetization were measured at several temperatures between 3 and 300 K (Fig. 3). At 300 K, both $M_{||}$ and $M_\perp$ show a linear behavior typical of a paramagnetic state. A small step in magnetization is observed

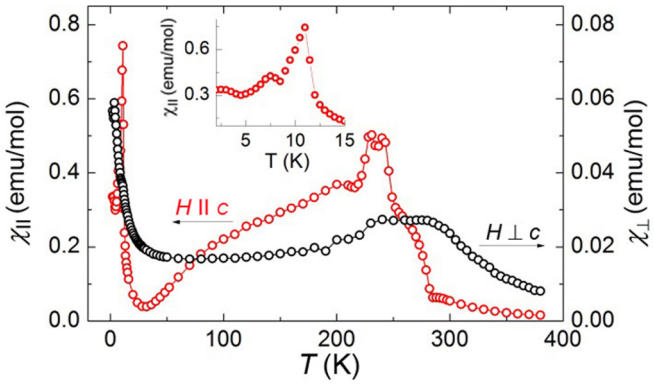

FIG. 2. Temperature dependence of magnetic susceptibility measured on a single crystal of $La_{0.25}Pr_{0.75}Co_2P_2$ in the field-cooled mode, with the magnetic field of 0.01 T applied parallel (red curve) and perpendicular (black curve) to the c axis. The inset shows an enlarged part of the $H||c$ dependence in the low-temperature region.

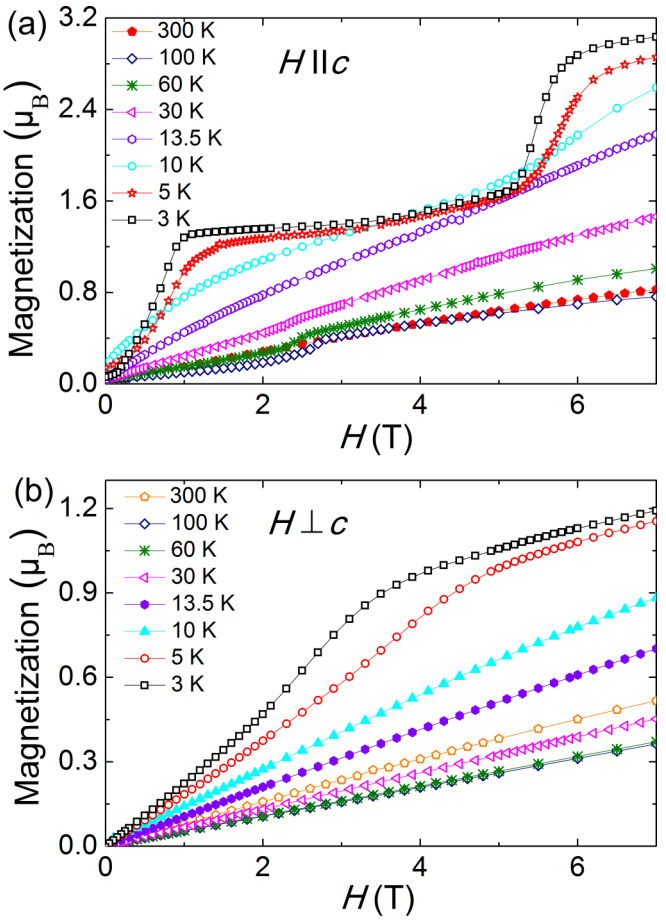

FIG. 3. Isothermal field dependences of magnetization for a single crystal of $La_{0.25}Pr_{0.75}Co_2P_2$ measured with the magnetic field parallel (a) and perpendicular (b) to the c axis.

around 2.5 T at 100 and 60 K, which suggests the breakdown of the Co AFM structure under applied magnetic field. The rather small value of magnetization observed above the critical field is in accord with the small Co moments observed previously in these materials (<0.5 μ_B per Co atom) [14,16]. This metamagnetic step, however, is not observed in the curves measured at 30, 13.5, and 10 K. The slope of these curves gradually increases as the temperature is lowered, due to the increased paramagnetic contribution from the Pr moments. The curves measured at 5 and 3 K exhibit a very different behavior, as we observe two metamagnetic transitions at the critical fields of 0.8 and 5.4 T with a plateaulike region between those field values. The larger magnetization values observed for these curves suggest field-induced transitions might involve reorientation of Pr spins. It is appropriate to note that we recently reported a similar two-step metamagnetic behavior for the isostructural $PrCo_2As_2$ and $NdCo_2As_2$ [24].

The $M_\perp$ curves exhibit smaller magnetization values, which agree with the *ab* plane being the hard magnetization direction. Nearly linear curves are observed between 300 and 10 K. The 100-K and 60-K lines have nearly the same slope, which is smaller than the slope of the 300-K line, in agreement with the AFM-ordered state. At lower temperatures, the slope gradually increases due to the increased contribution from the Pr moments. Finally, at 5 and 3 K, a deviation from the linear behavior is observed at higher magnetic fields, which suggests the AFM ordered Pr moments are canted by the applied field away from the easy axis.

C. Resistivity and magnetoresistance

The temperature dependence of electrical resistivity was measured in zero magnetic field. The resistivity decreases as the temperature is lowered, revealing a metallic behavior (Fig. 4). A sharp drop in resistivity occurs below 11 K, indicating that the AFM ordering of Pr moments greatly reduces the spin-dependent scattering of conducting carriers in the $[Co_2P_2]$ layer. This resistivity anomaly at the AFM transition temperature was also observed in other compounds with the $ThCr_2Si_2$ and related structure types [25–27].

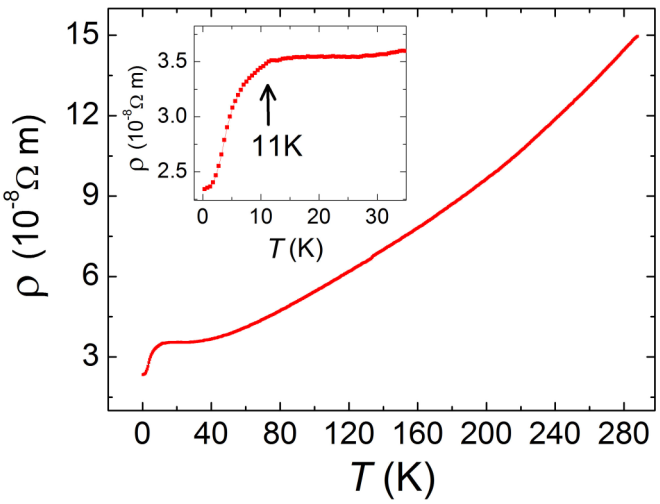

FIG. 4. Electrical resistivity measured on a single crystal of $La_{0.25}Pr_{0.75}Co_2P_2$. The inset shows an enlarged low-temperature range.

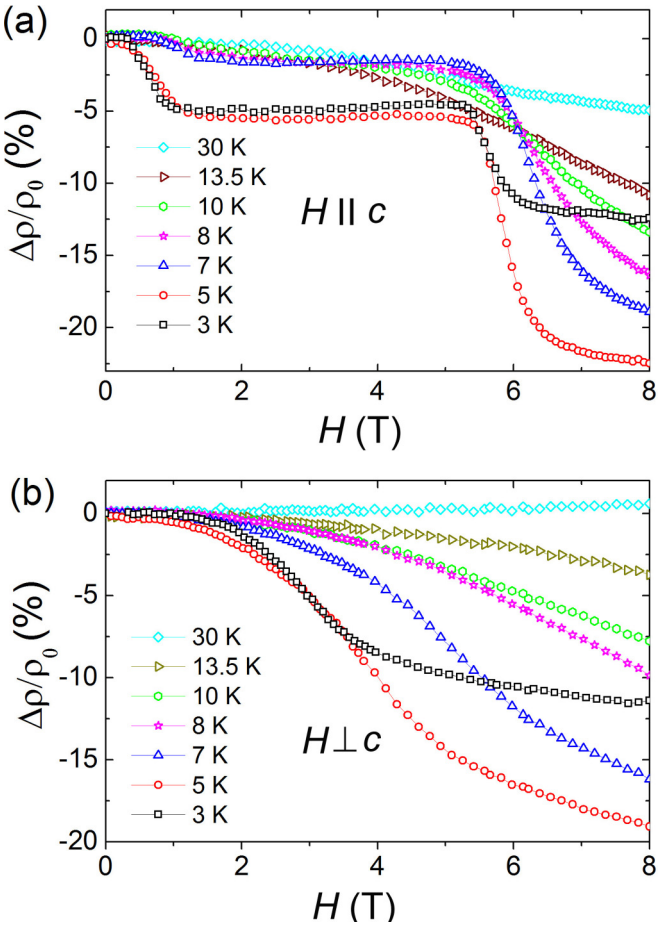

FIG. 5. Magnetoresistance measured on a single crystal of $La_{0.25}Pr_{0.75}Co_2P_2$ at various temperatures with the magnetic field applied parallel (a) and perpendicular (b) to the *c* axis.

To further investigate the metamagnetic transitions observed in the magnetic measurements at low temperatures, magnetoresistance (MR) measurements were conducted from 3 to 30 K with an applied magnetic field up to 8 T (Fig. 5). With $H||c$ at 3 K and 5 K, two sharp magnetoresistance drops are observed at 0.8 and 5.4 T, which are in excellent agreement with the two metamagnetic steps observed in field-dependent magnetization data [Fig. 3(a)]. Analogous to the giant magnetoresistance effect in ferromagnetic/nonmagnetic multilayers, the carrier transport in $La_{0.25}Pr_{0.75}Co_2P_2$ occurs mainly in the $[Co_2P_2]$ layers, and at low temperature the spin-dependent scattering stems primarily from the two layers of localized Pr^{3+} ions. As will be detailed in the next section, the external field induces the reorientation of the Pr moments in one of the layers which increasingly suppress the antialignment of the two sets of Pr moments, causing the decrease in spin-dependent scattering and negative MR. This is in contrast to the non-monotonic MR observed in $CeNi_2As_2$ [28], which does not exhibit a close correlation with the magnetization and is believed to originate from spin disorder scattering. The resistance drops become less obvious when the temperature is increased to 8–10 K and vanish at higher temperatures.

This behavior further supports the origin of MR from the Pr spins reorientation under magnetic field, since the MR drops (Fig. 5) and the metamagnetic steps [Fig. 3(a)] disappear simultaneously as the temperature is increased. It will be shown below that the applied field has no effect on the magnetic ordering in the Co sublattice at these temperatures. Similar to the case of $H||c$, the MR behavior for $H\perp c$ shows a close correlation with the field-dependent magnetization measured in the same direction. Because the Pr spins are harder to align in the ab plane than along the c axis, the MR with $H\perp c$ shows a less steep decrease below 10 K, and its magnitude is somewhat smaller than that observed with $H||c$ at the same magnetic field for all temperatures.

D. Magnetic structure

1. Neutron diffraction

The observation of multiple magnetic phase transitions in $La_{0.25}Pr_{0.75}Co_2P_2$ by magnetic measurements urged us to perform powder and single crystal neutron diffraction studies to establish the magnetic structures of this material under various temperature and magnetic field conditions. The unit cell parameters refined from powder neutron diffraction data (Table I) agree well with the parameters determined from single crystal x-ray diffraction data [14]. (The broad features observed in all diffraction patterns at 23° and 41° are due to intrinsic instrumental background, which was modeled by a linear interpolation between selected points.)

The neutron powder diffraction pattern obtained at 225 K does not show any additional reflections as compared to the pattern recorded at 300 K. According to magnetization measurements, $La_{0.25}Pr_{0.75}Co_2P_2$ exhibits a FM ordering of Co moments between 225 and 282 K, with the easy magnetization along the c axis [Fig. 7(a)]. This FM structure is expected to only modify intensities of the nuclear peaks, but due to the low magnetic moment per Co atom (see below) such enhancement could not be detected in the neutron powder diffraction pattern. Below 225 K, new Bragg peaks become visible. They were indexed with a propagation vector $\boldsymbol{k_1} = (0,0,1/2)$. Figure 6(a) shows the diffraction pattern measured at 30 K. The best refinement of this pattern with $\boldsymbol{k_1} = (0,0,1/2)$ is achieved for the magnetic structure in which Co spins align FM along the c axis within each $[Co_2P_2]$ layer, but the orientation of the spins with respect to the c axis is reversed in every two layers. Therefore the magnetic structure is AFM with a doubled c axis, as compared to the nuclear structure ($c_{magn} = 2c_{nucl}$) [Fig. 7(b)]. Such structure can be described by the magnetic space group P_c4cc (#103.200) [29] with the following atomic and magnetic configuration for Co atoms: $(0,1/2,1/8|0,0,m_z)$, $(1/2,0,1/8|0,0,m_z)$, $(0,1/2,5/8|0,0,-m_z)$, $(1/2,0,5/8|0,0,-m_z)$, $(1/2,0,3/8|0,0,m_z)$, $(0,1/2,3/8|0,0,m_z)$, $(1/2,0,7/8|0,0,-m_z)$, $(0,1/2,7/8|0,0,-m_z)$. The component of Co magnetic moment along the c axis, m_z, was refined to the value of $0.85(5)\,\mu_B$ at 30 K. The magnetic structure and the Co magnetic moment are similar to those established for $PrCo_2P_2$ at 304 K, with $m(Co) \sim 0.8\,\mu_B$ [13].

The appearance of additional magnetic reflections in the neutron powder diffraction patterns collected at 10 and 4 K

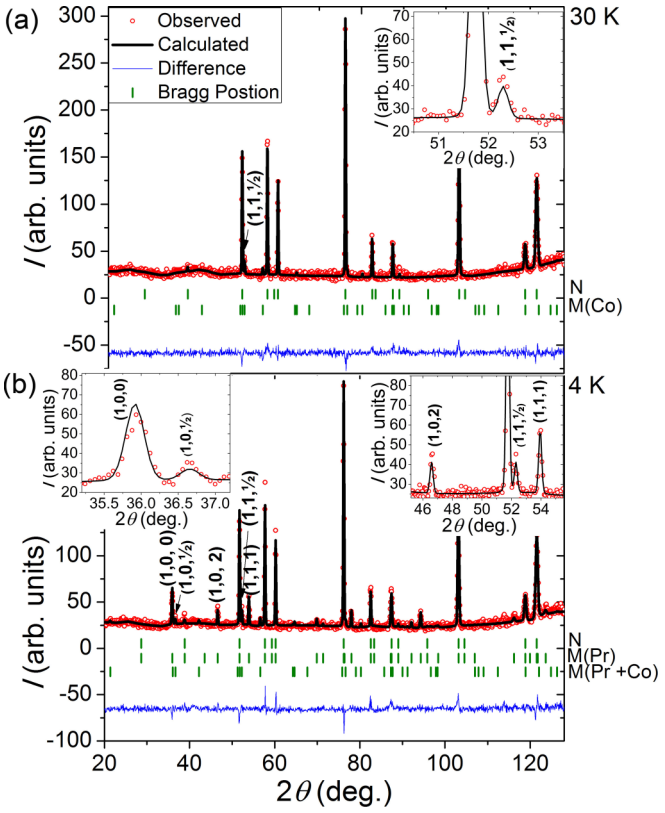

FIG. 6. Rietveld refinement of neutron powder diffraction patterns of $La_{0.25}Pr_{0.75}Co_2P_2$ collected at (a) 30 K and (b) 4 K. Magnetic peaks are emphasized in the insets.

[Figs. S2 and 6(b)] is likely associated with the AFM ordering of Pr moments. Both patterns showed magnetic reflections (1,0,0), (1,0,1/2), (1,0,2), (1,1,1/2), and(1,1,1), all of which are forbidden by the $I4/mmm$ symmetry of the nuclear structure. The (1,0,1/2) and (1,1,1/2) peaks were indexed with the propagation vector $\boldsymbol{k_1} = (0,0,1/2)$, while the (1,0,0), (1,0,2),

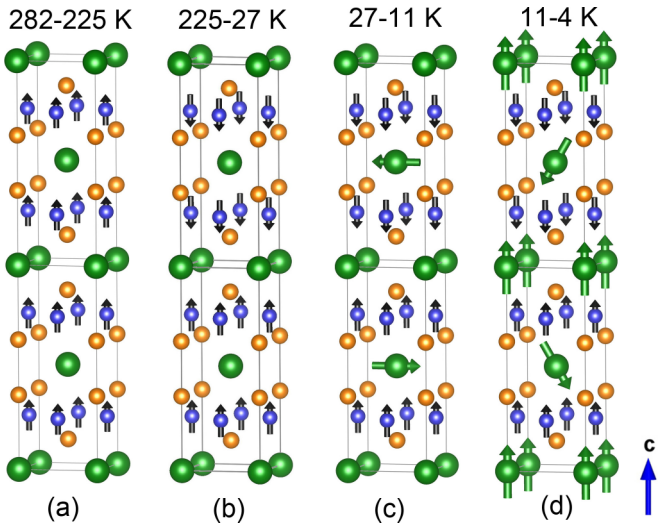

FIG. 7. Evolution of the magnetic structure of $La_{0.25}Pr_{0.75}Co_2P_2$ as a function of temperature: (a) 282–225, (b) 225–27, (c) 27–11, and (d) 11–4 K.

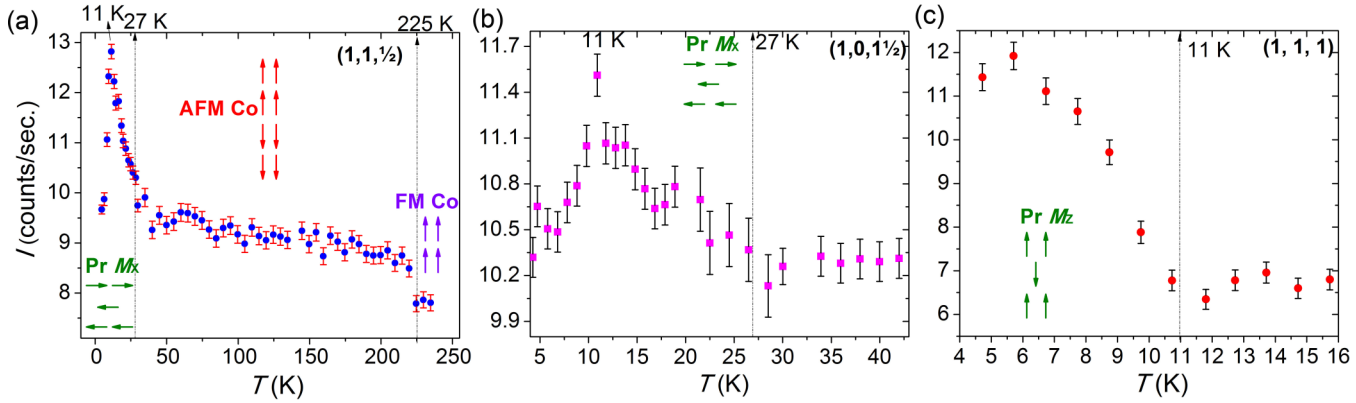

FIG. 8. Temperature dependence of intensities of (a) (1,1,½), (b) (1,0,1½), and (c) (1,1,1) magnetic peaks.

and (1,1,1) peaks were indexed with the propagation vector $\boldsymbol{k_2} = (1,0,0)$. The overall magnetic structure still has a doubled c axis relative to the nuclear structure.

To further confirm the indexing of magnetic peaks in the neutron powder diffraction data, additional diffraction experiments were performed on a single crystal of $La_{0.25}Pr_{0.75}Co_2P_2$. The intensity of the (1,1,½) magnetic peak was monitored as a function of temperature [Fig. 8(a)]. The increase in the intensity below 225 K can be ascribed to the FM → AFM transition in the Co sublattice, which is consistent with the AFM model refined from the neutron powder diffraction data at 30 K. Below 27 K, the intensity increases gradually to reach a maximum at 11 K. As the temperature is decreased below 11 K, the intensity of the (1,1,½) peak decreases dramatically but remains within the detection range at 5 K. Magnetic peaks (1,0,1½) and (0,0,1½), which are also associated with $\boldsymbol{k_1} = (0,0,½)$, exhibit significant intensity only below 27 K and also follow behavior similar to that of (1,1,½) at low temperatures [Figs. 8(b) and S3)]. It should be noted that the existence of the (0,0,1½) peak also rules out the possibility that the Pr moments with the propagation vector $\boldsymbol{k_1} = (0,0,½)$ order parallel to the c axis. In contrast to the $\boldsymbol{k_1}$-related magnetic peaks, the (111) magnetic peak associated with the second wave vector, $\boldsymbol{k_2} = (1,0,0)$, develops only bellow 11 K and follows a power-law temperature dependence down to the lowest measured temperature of 5 K [Fig. 8(c)].

Based on these observations, we attributed the wave vector $\boldsymbol{k_1}(0,0,½)$ to the in-plane magnetically ordered component that starts to develop on the Pr sites around 27 K. The profile of the order parameter of this transition (Fig. 8(a)) is not of the power-law-type, $(1–T/T_n)^{\beta}$, but rather exhibits an exponential growth that indicates a gradual progression from the short-range to long-range ordering of Pr moments. The increase in the intensity of magnetic reflections below 27 K also matches very well the gradual increase in the χ values observed around the same temperature for both orientations of the magnetic field (Fig. 2).

Below 11 K, an additional magnetic component with the wave vector $\boldsymbol{k_2}(1,0,0)$ appears along the c axis, while the in-plane component diminishes. The sequential magnetic ordering of Pr moments can be understood by considering the different molecular fields induced by the ordered Co moments at the Pr sites at the corners and at the center of the nuclear unit cell. One can expect the moment at the body-centered position to develop earlier. Such a sequential order is also consistent with the increase in magnetic susceptibility below 30 K and the maximum at 11 K observed in magnetic measurements (Fig. 2).

The diffraction data acquired between 11 and 27 K can be satisfactorily explained using only $\boldsymbol{k_1} = (0,0,½)$ for the ordering of both Co and Pr moments, described by the magnetic space group C_c2/c (No. 15.90) [29]. Within this symmetry, the Co atoms preserve the AFM order along the c axis, while only half of the Pr atoms develop an ordered moment. The Pr atomic coordinates and the associated magnetic moments within the magnetic unit cell ($a = b$, $c_{magn} = 2c_{nucl}$) are the following: Pr1 (0,0,0|0,0,0), (0,0,½|0,0,0) and Pr2 (½,½,¼|m_x,m_x,m_z), (½,½,¾|–m_x,–m_x,–m_z), corresponding to the corner and body-center sites, respectively, in the nuclear unit cell. Note that only the Pr2 atoms carry ordered magnetic moments. This intermediate magnetic structure is depicted in Fig. 7(c).

As mentioned earlier, for temperatures below 11 K the magnetic structure model for the Pr sublattice needs to include a second propagation vector, $\boldsymbol{k_2}(1,0,0)$, which accounts for the ordering of the m_z moment component. Such ordering breaks the body-centering translation symmetry and implies that the Pr1 moments are oriented antiparallel to the Pr2 moments. As a result, the overall magnetic structure at 4 K consists of layers of Pr moments with a magnetic m_z component that alternates orientation every layer along the c axis, while the m_x components are present and alternate orientation only every other layer [Fig. 7(d)]. The refined Co moment at 4 K is 0.87(4) μ_B, similar to the value obtained at 30 K. In the case of Pr, the refinement led to $m_z = 2.47(4)\,\mu_B$ and $m_x = 1.4(1)\,\mu_B$. Thus, the total Pr moment is 2.47(4) μ_B at the Pr1 (0,0,0) site and 3.1(1) μ_B at the Pr2 (½,½,¼) site, while the theoretical expectation value, calculated with the Lande g-factor of 0.8 for the $Pr^{3+}(4f^2)$ ion, is 3.2 μ_B.

2. Neutron diffraction in applied magnetic field

To elucidate the stepwise transitions observed in field-dependent magnetization data, we performed neutron powder diffraction under applied magnetic field. The measurements were carried out using fresh samples pressed into pellets to

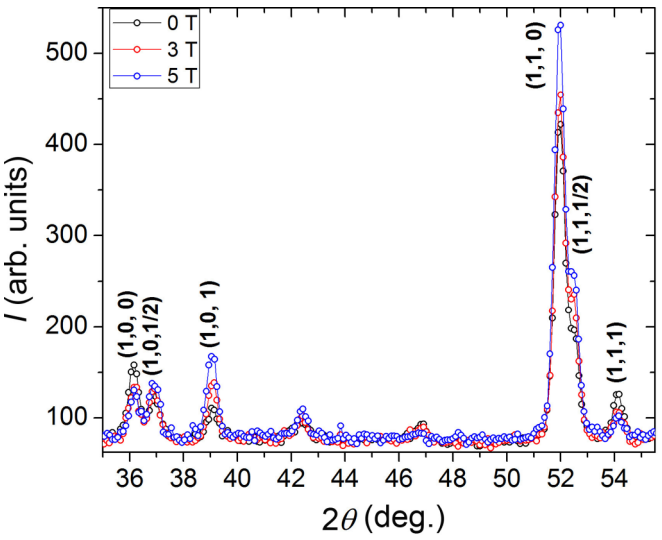

FIG. 9. Part of the neutron powder diffraction patterns of $La_{0.25}Pr_{0.75}Co_2P_2$ collected at 3 K under applied magnetic fields of 0, 3, and 5 T.

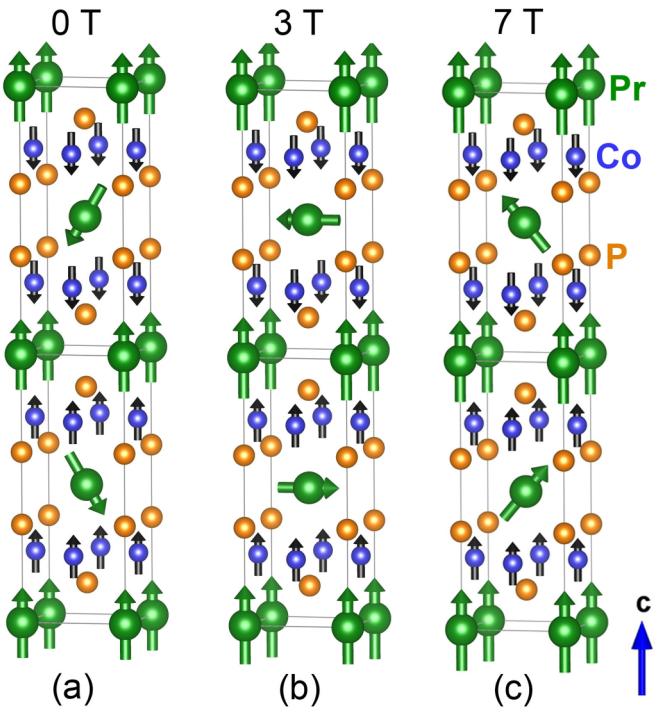

FIG. 10. Magnetic structure models of $La_{0.75}Pr_{0.25}Co_2P_2$ in different applied magnetic fields.

avoid powder grains reorientation in the applied magnetic field. Since the sample exhibits strong magnetic anisotropy, we are discussing the evolution of the magnetic moments under applied field only qualitatively. The diffraction patterns collected at 3 K in magnetic fields of 3 and 5 T (Fig. 9) revealed all magnetic peaks that were observed in the diffraction patterns recorded in zero field. A fit of data obtained in zero field was carried out using the same model as described above [Fig. 7(d)], i.e. AFM ordered Co moments along the c axis and AFM ordered Pr moments with m_x ($\boldsymbol{k_1} = (0,0,1/2)$) and m_z ($\boldsymbol{k_2} = (1,0,0)$) components [Fig. 10(a)].

When a 3-T magnetic field is applied, the intensity of the $(1,0,1/2)$ peak, related to the AFM ordered m_x(Pr) component, remains unchanged, while the intensities of the (1,0,0) and (1,1,1) peaks, related to the AFM ordered m_z(Pr) component, decrease with respect to the zero-field values. In contrast, the (1,0,1) and (1,1,0) nuclear peaks show a notable increase in intensities. The presence of magnetic scattering at these Bragg reflections is strongly suggestive of a magnetic order where the m_z components of Pr moments located in successive layers are no longer compensating. Specifically, the canted moments of Pr2 atoms located at $(1/2,1/2,1/4)$ in the magnetic unit cell ($c_{magn} = 2c_{nucl}$) may undergo a spin-flop transition to a state in which they lie approximately in the ab plane, and thus offer no compensation to the m_z moments of Pr1 atoms located at (0,0,0) [Fig. 10(b)]. This model, consisting of Pr1 moments along the c axis and Pr2 moments locked in the ab plane, is fully consistent with the plateau observed in the bulk magnetization measurements [Fig. 3(a)]. The plateau $M_{||}$ value of 1.4 μ_B per Pr atom is close to the half of the refined m_z projection of Pr1 moment in zero magnetic field.

Diffraction data measured at 5 T show an increase in the intensity of the (1,0,1) and (1,1,0) FM-type peaks. One can assume that at higher fields the Pr moments are forced to realign towards the c axis, which eventually results in the second magnetization plateau with the onset at ~6 T [Fig. 3(a)]. Meanwhile, the Co moments remain AFM ordered [Fig. 10(c)]. Such a high-field magnetic structure model is again consistent with the $M_{||}$ value of ~2.9μ_B observed at 7 T, but it requires further confirmation by neutron diffraction studies in stronger fields.

3. *Comparison to* $PrCo_2P_2$ *in applied magnetic field*

The unusual behavior of $La_{0.25}Pr_{0.75}Co_2P_2$ under applied magnetic field incited us to re-investigate the parent compound $PrCo_2P_2$, in which both Pr and Co moments show AFM ordering [13]. When the magnetic field is applied along the c axis of a single crystal of $PrCo_2P_2$, we also observe two steps in the field-dependent magnetization curve (Fig. 11). The first, smaller step occurs at ~0.1 T and the second, larger sharp step occurs at 5.5 T. A linear behavior typical of an antiferromagnetic state is observed with the field applied in the ab plane, suggesting the c axis is the easy magnetization direction for $PrCo_2P_2$, as has been confirmed by earlier neutron diffraction experiments in zero magnetic field [13].

Similar to the neutron diffraction experiments on $La_{0.25}Pr_{0.75}Co_2P_2$, we pelletized ~7 g of polycrystalline $PrCo_2P_2$. The sample was studied in applied magnetic fields up to 7 T. The neutron diffraction pattern collected at 1.5 K and 0 T shows many strong magnetic peaks due to AFM ordering of Pr and Co moments (Fig. S4). The refinement indicates that the AFM ordered Pr moments with the propagation vector $\boldsymbol{k_2} = (1,0,0)$ contribute to such peaks as (1,0,0) and (1,0,2) while the AFM ordered Co moments with the propagation vector $\boldsymbol{k_1} = (0,0,1/2)$ contribute to peaks such as $(1,1,1\,1/2)$. The refined moments are 2.75(9) μ_B for Pr and 0.82(1) μ_B for Co. Note that no in-plane ordered component has been observed for this material in zero magnetic field. These results,

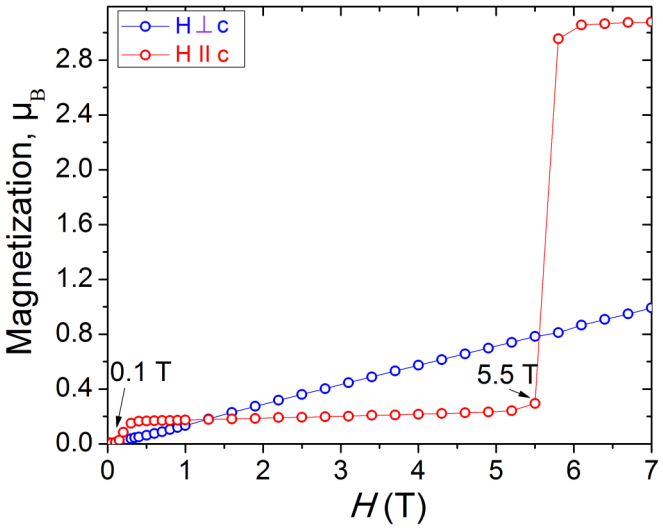

FIG. 11. Field dependence of magnetization for a single crystal of $PrCo_2P_2$ measured with the magnetic field applied parallel (red) and perpendicular (blue) to the c axis.

as well as the refined magnetic structure [Fig. 12(a)], match well with the previous report by Jeitschko *et al.* [13].

Since the sample exhibits strong magnetic anisotropy, we are again discussing the evolution of its magnetism under applied field only qualitatively. At an intermediate field of 3.5 T, some additional magnetic scattering is observed for the (1,0,1) and (1,1,0) peaks (Fig. S5), due to the presence of noncompensating Pr moments at the ($^1/_2$,$^1/_2$,$^1/_4$) and (0,0,0) positions of the magnetic unit cell. This behavior is very similar to that seen in $La_{0.25}Pr_{0.75}Co_2P_2$, but without any detectable canting of Pr moments away from the c-axis. The corresponding magnetic structure model is displayed in Fig. 12(b). When the magnetic field is increased to 7 T, new magnetic peaks described by the propagation vector $\boldsymbol{k_1} = (0,0,^1/_2)$ also appear in the pattern (Fig. S5), providing a signature of a spin-flop-like transition with an additional AFM component of Pr moments appearing in the ab plane. Given the magnetic structure of $PrCo_2P_2$ at lower fields and the resemblance of the scattering profile to that observed for $La_{0.25}Pr_{0.75}Co_2P_2$, it is reasonable to assume that the m_x moment component emerges from the rotation away from the c axis of only the Pr moments in the ($^1/_2$,$^1/_2$,$^1/_4$) position as the stronger magnetic field breaks their collinear AFM arrangement relative to the Pr moments in the (0,0,0) position [Fig. 12(c)]. We relate this rotation to the second magnetization jump that takes place at 5.5 T (Fig. 11). The saturation moments per Pr atom achieved at 7 T in $PrCo_2P_2$ and $La_{0.25}Pr_{0.75}Co_2P_2$ are nearly the same, $\sim 2.9\mu_B$, and therefore, we believe that these compounds have the same magnetic structures at this magnetic field.

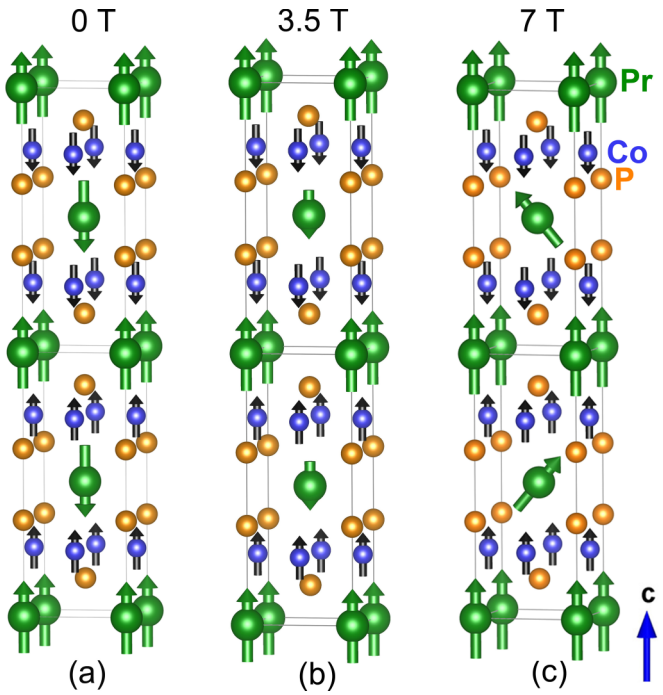

FIG. 12. Magnetic structure models of $PrCo_2P_2$ with applied magnetic fields up to 7 T at 1.5 K.

IV. CONCLUDING REMARKS

In contrast to the rather simple magnetism of ternary phosphides $LaCo_2P_2$ and $PrCo_2P_2$, the intermediate quasiquaternary phase $La_{0.25}Pr_{0.75}Co_2P_2$ demonstrates more complex magnetic behavior as confirmed by magnetic, magnetoresistance, and neutron diffraction measurements on single-crystal and powder samples. $La_{0.25}Pr_{0.75}Co_2P_2$ exhibits FM ordering around 282 K due to Co spins aligning along the c axis, which is different from both the FM ordering of Co moments in the ab plane at 132 K in $LaCo_2P_2$ and the AFM ordering of Co moments along the c axis at 309 K in $PrCo_2P_2$. Nevertheless, at 225 K the Co sublattice in $La_{0.25}Pr_{0.75}Co_2P_2$ does undergo another phase transition that results in the AFM ordering of Co moments with doubling of the c axis in the magnetic unit cell, analogous to the AFM structure of $PrCo_2P_2$.

Similar to the magnetic behavior of $PrCo_2P_2$, the Pr moments in $La_{0.25}Pr_{0.75}Co_2P_2$ also exhibit ordering at lower temperatures. However, while only one AFM phase transition is observed for $PrCo_2P_2$ at 19 K, the Pr moments in $La_{0.25}Pr_{0.75}Co_2P_2$ undergo two sequential AFM transitions at 27 and 11 K. In zero magnetic field, the higher-temperature transition is associated with the AFM ordering of a half of Pr moments in the ab plane [Fig. 7(c)] and the lower-temperature transition is caused by the AFM ordering of the other half of Pr moments along the c axis and canting of the previously ordered Pr moments toward the c axis while maintaining the overall AFM ordered arrangement [Fig. 7(d)]. Such canting is not observed in the magnetic structure of $PrCo_2P_2$ [Fig. 12(a)].

This difference in the temperature-dependent properties of the Pr sublattice in $PrCo_2P_2$ and $La_{0.25}Pr_{0.75}Co_2P_2$ is also reflected the behavior of these compounds under applied magnetic field. In zero field at the lowest temperature of our experiments both compounds exhibit similar AFM structures, with the only difference being partial canting of a half of Pr moments away from the c axis in $La_{0.25}Pr_{0.75}Co_2P_2$ [cf. Figs. 10(a) and 12(a)]. Under applied field, the moment on one of the two crystallographically unique Pr sites in the magnetic unit cell of $PrCo_2P_2$ is gradually suppressed [Fig. 12(b)]

until an abrupt metamagnetic step occurs at 5.5 T due to the reorientation of the Pr moments to adopt the FM ordered structure, with a half of the moment being parallel and the other half canted with respect to the *c* axis [Fig. 12(c)]. $La_{0.25}Pr_{0.75}Co_2P_2$, on the other hand, shows two successive metamagnetic transitions in the Pr sublattice. The first one, at 0.8 T, is due to the spin-flop-like reorientation of the canted Pr moments into an AFM ordered arrangement parallel to the *ab* plane [Fig. 10(b)], which is not observed for $PrCo_2P_2$. The second transition, at 5.4 T, is associated with further reorientation of these moments toward the *c* axis to adopt the FM structure [Fig. 10(c)], essentially similar to that observed for $PrCo_2P_2$ above 5.5 T [Fig. 12(c)].

We have previously shown that maintaining the FM ordering in the Co sublattice to lower temperatures results in the antiparallel coupling of the $3d$ and $4f$ moments and FiM ground state for $La_{0.75}Pr_{0.25}Co_2P_2$. In $La_{0.25}Pr_{0.75}Co_2P_2$, however, the initial FM ordering of Co moments breaks down at 225 K, causing a magnetic behavior that is more reminiscent of $PrCo_2P_2$. Given the fact that the relatively small structural changes between these quasi-quaternary phases result in such dramatic modification of magnetic behavior, it is of interest to carry out detailed investigation of magnetic behavior for intermediate compositions, e.g., $La_{0.5}Pr_{0.5}Co_2P_2$. We will report results of such studies in due course.

ACKNOWLEDGMENTS

We thank the U.S. National Science Foundation for the support of this work through awards DMR-0955353 and DMR-1507233 to M.S. and DMR-1308613 to P.X. Experiments at the Oak Ridge National Laboratory's High Flux Isotope Reactor were sponsored by the Scientific User Facilities Division, Office of Basic Energy Sciences, US Department of Energy (DOE).

[1] R. Hoffmann and C. Zheng, J. Phys. Chem. **89**, 4175 (1985).
[2] S. M. Kauzlarich, in *Chemistry, Structure, and Bonding of Zintl Phases and Ions*, edited by S. M. Kauzlarich (Wiley-VCH, New York, 1996), p. 245.
[3] R. T. Macaluso and B. K. Greve, Dalton Trans. **41**, 14225 (2012).
[4] A. Szytuła and J. Leciejewicz, in *Handbook on the Physics and Chemistry of Rare Earths*, edited by K. A. Gschneidner, Jr. and L. Eyring (North-Holland, Amsterdam, 1989), Vol. 12, p. 133.
[5] F. Steglich, J. Aarts, C. D. Bredl, W. Lieke, D. Meschede, W. Franz, and H. Schäfer, Phys. Rev. Lett. **43**, 1892 (1979).
[6] M. Rotter, M. Tegel, and D. Johrendt, Phys. Rev. Lett. **101**, 107006 (2008).
[7] P. C. Canfield and S. L. Bud'ko, Annu. Rev. Condens. Matter Phys. **1**, 27 (2010).
[8] H. S. Jeevan, Z. Hossain, D. Kasinathan, H. Rosner, C. Geibel, and P. Gegenwart, Phys. Rev. B **78**, 092406 (2008).
[9] Y. P. Qi, Z. S. Gao, L. Wang, D. L. Wang, X. P. Zhang, and Y. W. Ma, New J. Phys. **10**, 123003 (2008).
[10] M. Reehuis and W. Jeitschko, J. Phys. Chem. Solids **51**, 961 (1990).
[11] M. Reehuis, C. Ritter, R. Ballou, and W. Jeitschko, J. Magn. Magn. Mater. **138**, 85 (1994).
[12] M. Reehuis, W. Jeitschko, G. Kotzyba, B. Zimmer, and X. Hu, J. Alloys Compd. **266**, 54 (1998).
[13] M. Reehuis, P. J. Brown, W. Jeitschko, M. H. Möller, and T. Vomhof, J. Phys. Chem. Solids **54**, 469 (1993).
[14] K. Kovnir, C. M. Thompson, H. D. Zhou, C. R. Wiebe, and M. Shatruk, Chem. Mater. **22**, 1704 (2010).
[15] K. Kovnir, V. O. Garlea, C. M. Thompson, H. D. Zhou, W. M. Reiff, A. Ozarowski, and M. Shatruk, Inorg. Chem. **50**, 10274 (2011).
[16] K. Kovnir, C. M. Thompson, V. O. Garlea, D. Haskel, A. A. Polyanskii, H. D. Zhou, and M. Shatruk, Phys. Rev. B **88**, 104429 (2013).
[17] C. M. Thompson, K. Kovnir, V. O. Garlea, E. S. Choi, H. D. Zhou, and M. Shatruk, J. Mater. Chem. C **2**, 7561 (2014).
[18] V. O. Garlea, B. C. Chakoumakos, S. A. Moore, G. B. Taylor, T. Chae, R. G. Maples, R. A. Riedel, G. W. Lynn, and D. L. Selby, Appl. Phys. A **99**, 531 (2010).
[19] B. C. Chakoumakos, H. B Cao, F. Ye, A. D. Stoica, M. Popovici, M. Sundaram, W. Zhou, J. S. Hicks, G. W. Lynn, and R. Riedel, J. Appl. Crystallogr. **44**, 655 (2011).
[20] J. Rodríguez-Carvajal, Physica B **192**, 55 (1993).
[21] A. S. Wills, Physica B **276–278**, 680 (2000).
[22] J. M. Perez-Mato, S. V. Gallego, E. S. Tasci, L. Elcoro, G. de la Flor, and M. I. Aroyo, Annu. Rev. Mater. Res. **45**, 217 (2015).
[23] See Supplemental Material at http://link.aps.org/supplemental/10.1103/PhysRevB.95.024428 for additional magnetic and neutron diffraction plots and the Rietveld refinement of neutron diffraction patterns.
[24] C. M. Thompson, X. Tan, K. Kovnir, V. O. Garlea, A. A. Gippius, A. A. Yaroslavtsev, A. P. Menushenkov, R. V. Chernikov, N. Büttgen, W. Krätschmer, Y. V. Zubavichus, and M. Shatruk, Chem. Mater. **26**, 3825 (2014).
[25] S. A. Jiang, H. Xing, G. F. Xuan, Z. Ren, C. Wang, Z. A. Xu, and G. H. Cao, Phys. Rev. B **80**, 184514 (2009).
[26] C. Wang, L. Li, S. Chi, Z. Zhu, Z. Ren, Y. Li, Y. Wang, X. Lin, Y. Luo, S. Jiang, X. Xu, G. Cao, and Z. Xu, Europhys. Lett. **83**, 67006 (2008).
[27] A. Marcinkova, D. A. M. Grist, I. Margiolaki, T. C. Hansen, S. Margadonna, and J. W. G. Bos, Phys. Rev. B **81**, 064511 (2010).
[28] Y. Luo, J. Bao, C. Shen, J. Han, X. Yang, C. Lv, Y. Li, W. Jian, B. Si, C. Feng, J. Dai, G. Cao, and Z.-a. Xu, Phys. Rev. B **86**, 245130 (2012).
[29] D. B. Litvin, Acta Crystallogr. Sect. A, **A57**, 729 (2001).